Modularized, Reconfigurable and Bidirectional Charging Infrastructure for Electric Vehicles with Silicon Carbide Power Electronics (MoReSiC)

Deliverable D6.3 (Month 42)

Title: "The complete EV charging system extended by PV DC-DC rated up to 10 kW"

Authors: Krzysztof Kalinowski, Rafał Miśkiewicz, Grzegorz Wrona, Przemysław Trochimiuk, Rafał Kopacz, Jacek Rąbkowski, Warsaw University of Technology; Kaushik Naresh Kumar, Dimosthenis Peftitsis, NTNU; Radosław Sobieski, Markel;

NTNU
Norwegian University of Science and Technology

ICELAND LIECHTENSTEIN NORWAY
eea grants
norway grants

Warsaw University of Technology

Executive summary

The deliverable includes the description of complete experimental tests of the advanced EV charging system in all considered operation modes. This includes basic scenarios with the grid converter, EV isolated dc-dc converters, and the non-isolated dc-dc converter for the battery energy storage interfacing, as well as the cooperation with the additional dc-dc converter included for PV integration. The considered operation modes include slow charging of EVs via the grid (mode A), slow charging of EVs via the grid and the battery energy storage (mode B), fast charging of an EV from the grid with several converters in parallel (mode C), grid support with the power drawn from the energy storage (mode D), grid support from the EVs (mode E), island operation with the power flowing from the energy storage to the EVs (mode F). Furthermore, these are expanded with the additional operating modes possible with the inclusion of the PV converter (noted as +/−). In summary, all considered modes are performed in experiments, validating the concept and experimental models of the advanced charging station.

Table of Contents

1. The advanced EV charging station

The whole advanced electric vehicle (EV) charging system consists of four types of bidirectional power electronics converters: a three-level active rectifier with a three-port DC output to interface with a 3-phase grid, non-isolated three-level DC/DC converter interfacing energy storage (ES), isolated DC/DC converters interfacing EVs, and a unidirectional, three-level, non-isolated DC/DC converter. The block diagram of the full advanced EV charging system is presented in Figure 1. The system is explained in detail in D6.1 and shown here only for a quick reference for the experiments for each operation mode.

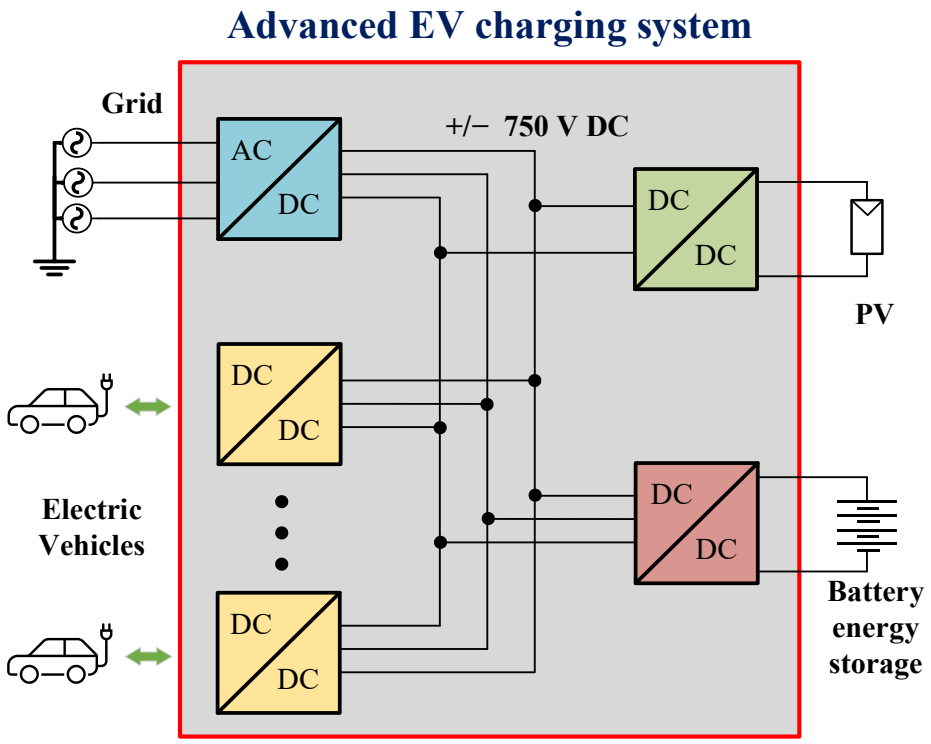

Fig. 1 Scheme of the advanced EV charging system.

2. Operation modes

In this section, experimental results will be shown for each operation mode and discussed on, exhibiting the possibilities of the station and validating the experimental model of the system.

a) Mode A: slow EV charging from the grid

In this mode, two converters are employed, the grid converter and EV converters (one or two). An exemplary result is depicted in Fig. 2, where a single EV converter is charged with up to 10 kW of power. Here, a common battery charging CC (constant current)-CV (constant voltage) characteristic is emulated. As can be seen, the power is slowly rising, until it reaches a maximum value of 10 kW, then, for a certain amount of time, constant current is delivered. Later, after the battery SOC (state of charge) reports higher values, the mode shifts to CV, and thus, the power is slowly lowered.

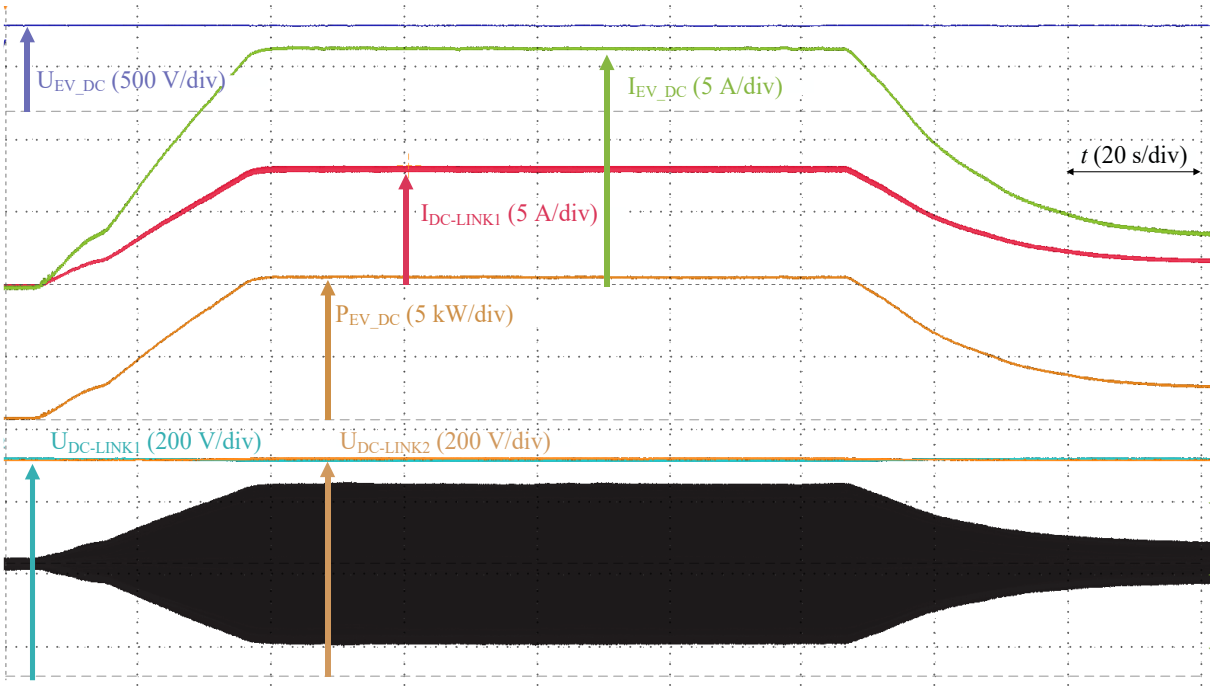

Fig. 2 An emulation of CC-CV charging of a single EV with one EV converter with the power drawn from the grid (up to 10 kW).

The efficiency characteristics in this scenario, for two different DC-link voltages of 1500 and 1200 V, are depicted in Fig. 3. As can be observed, higher voltage becomes more efficient at higher power ratings. All in all, given that this is two-stage conversion, the efficiency is a satisfactory level. Furthermore, it is worth noting that the experimental model is scaled, and in actual application with several hundred of kWs the efficiency would be higher.

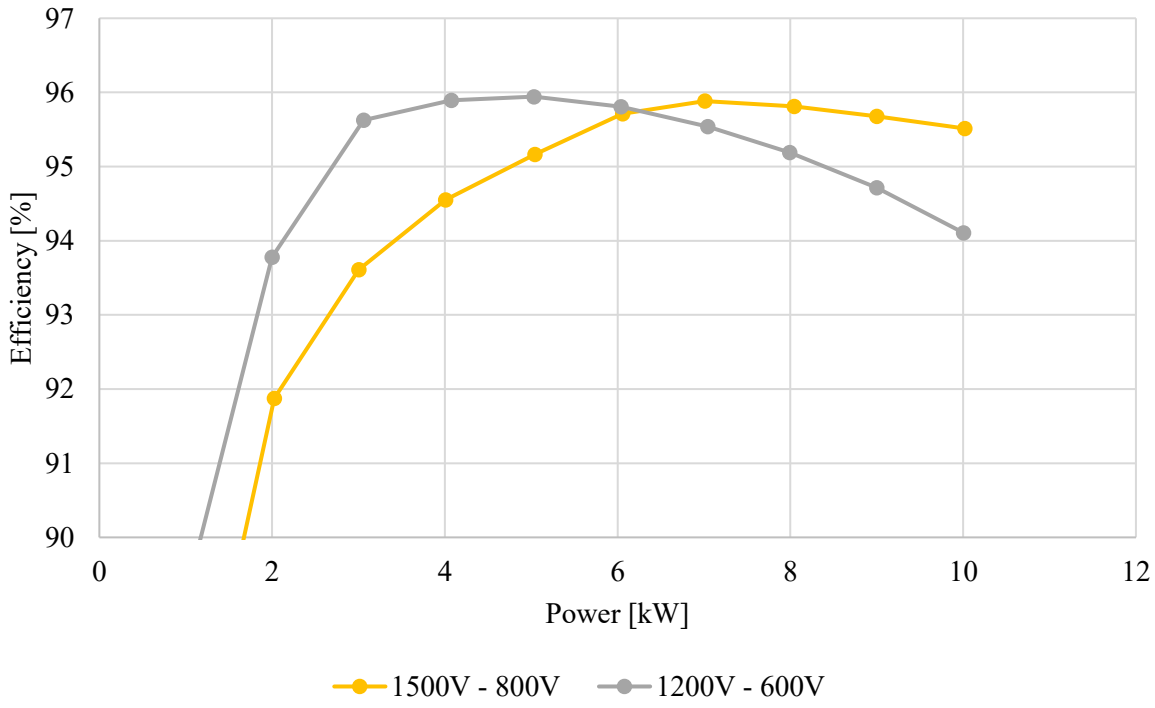

Fig. 3 Efficiency characteristics of single EV charging the power drawn from the grid (up to 10 kW).

Another possible scenario within this mode is depicted in Fig. 4. Here, the employed converters stay the same. However, another EV converter is employed to maximize the possible power drawn from the grid (up to 20 kW). Thus, according to the results in Fig. 4, the CC-CV charging processes are emulated for each EV separately. Therefore, at an overlap area, the momentary power reaches 20 kW.

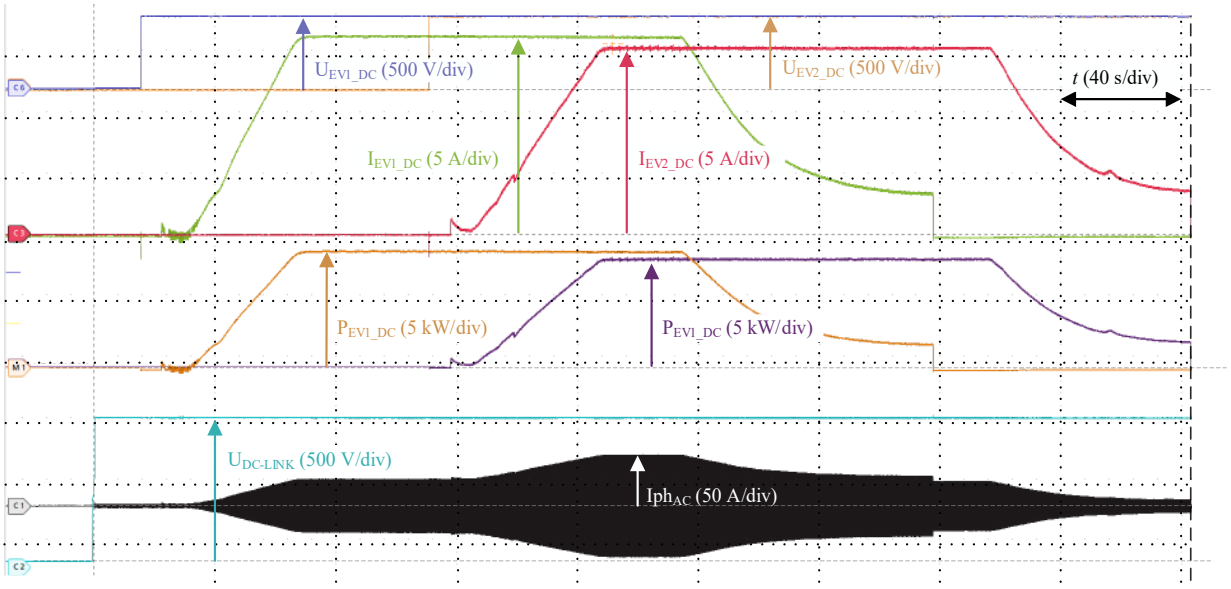

Fig. 4 An emulation of CC-CV charging of a two separate EV with two independent EV converters with the power drawn from the grid (up to 20 kW).

Finally, Fig. 5 depicts the THD of the grid current at different power levels. As can be seen, the minimum value is less than 4%, whereas it stays below 5% for roughly the upper half of the power characterstics. The higher THD at low powers appear because of the relatively low power of the scaled experimental model. For a full-scale converter to be applied in a real charging station with the power of hundreds of kWs, the THD would easily stay at very low levels for the majority of the power range, and thus, this would not be an issue. Nevertheless, the THD is already decent for the scaled model for most of the operating range.

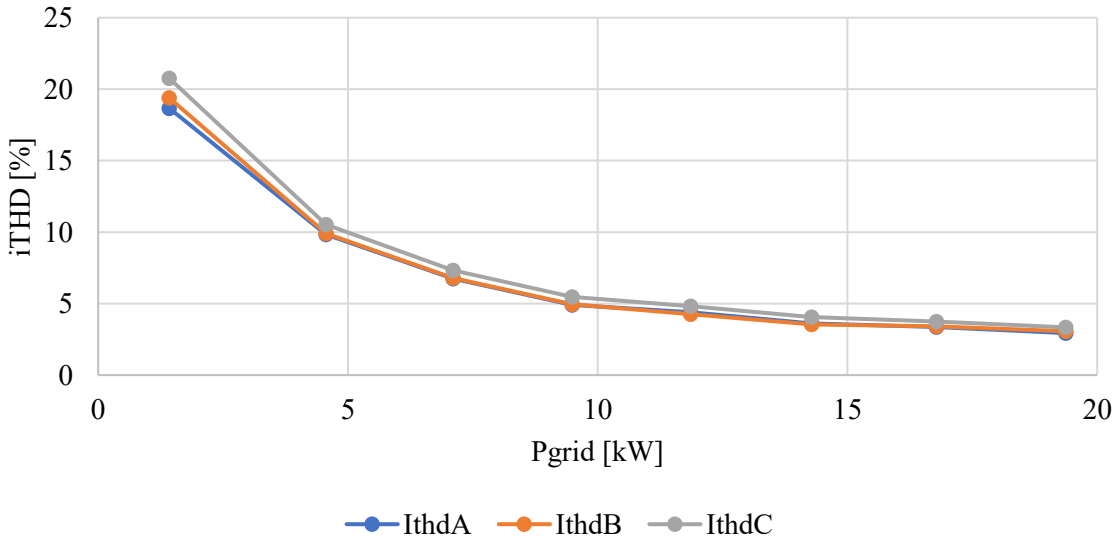

Fig. 5 THD of the grid current for various power levels.

b) Mode A+ slow EV charging from the grid with PV support

In this mode, the previous mode is expanded with the power being partially drawn from the PV, and the grid is not the sole source of energy. An exemplary result is depicted in Fig. 6. While the power share can vary, e.g., due to shift in sun conditions affecting PV energy generation, this specific oscillogram depicts a situation when the power draw split is even ($P_{grid} = P_{PV} = 5$ kW). However, the variation in the power split between the sources is visualized in Fig. 7. Here, the EV is charged with a constant power of 10 kW, and the power split for the PV plant and the grid is changing depending on the specific experimental sample (scenario), from 0 to 10 kW. Furthermore, this Fig. 7 also contains the efficiency measurement for each sample.

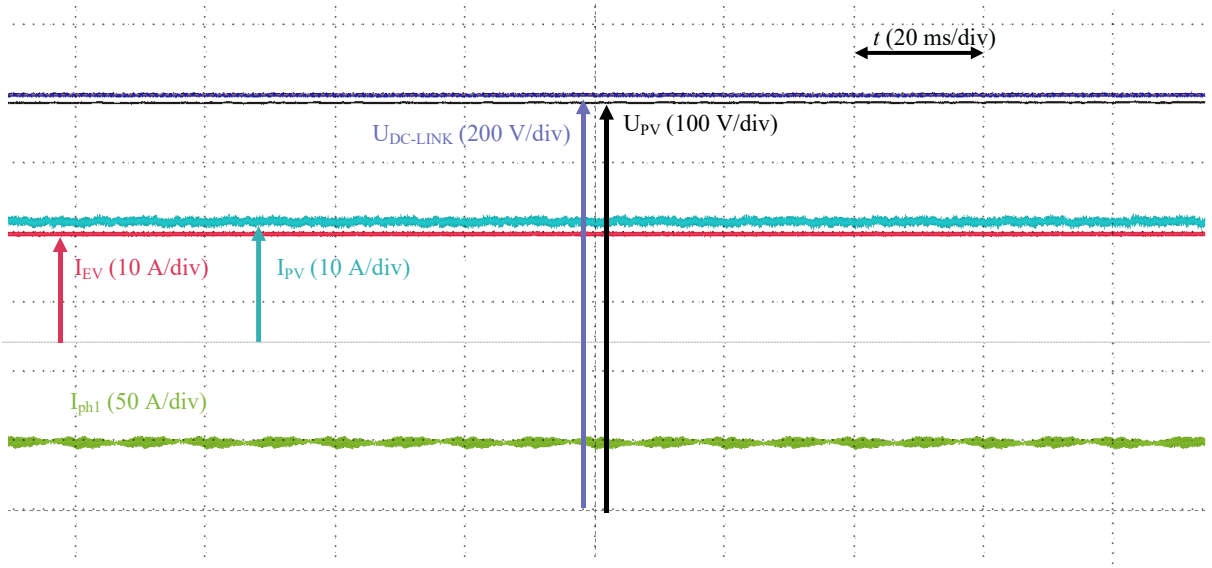

Fig. 6. Exemplary results from mode A+, with the power delivered from the grid (5 kW) and PV (5 kW) to the EV (10 kW).

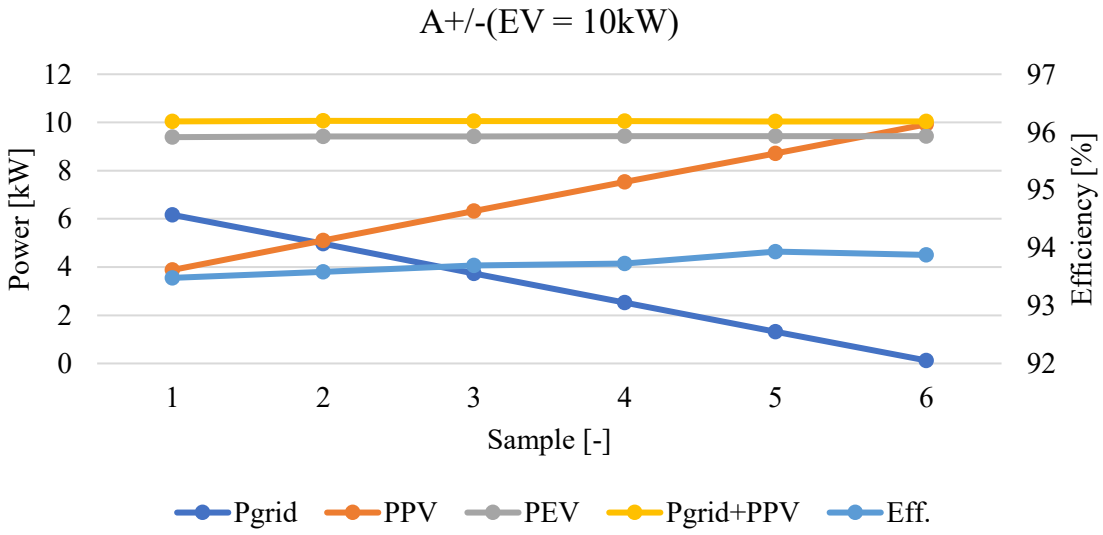

Fig. 7. Power characteristic in mode A/A+/A−, with the power split varying between the PV plant and the grid (0-10 kW) at a constant load power delivered to the EV at 10 kW.

c) Mode A- slow EV charging from the PV

In this mode, the assumption is that the PV delivers the power to the EV alone, and the grid converter is off. While this mode has already been partially covered in Fig. 7, it is further expanded with Fig. 8, where the efficiency is plotted for the power varying from 2 to 10 kW. Again, considering two-stage conversion, the achieved efficiency is decent.

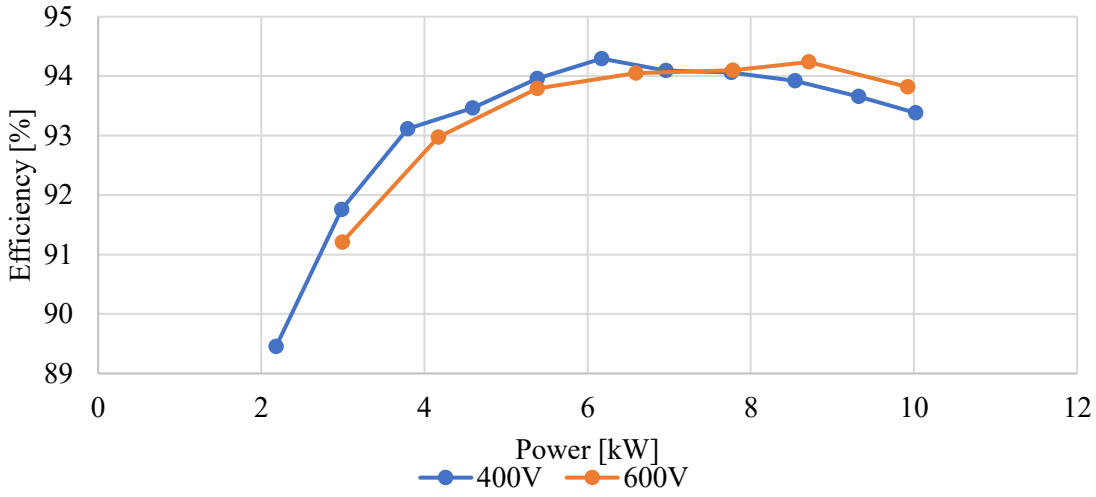

Fig. 8. Efficiency vs. power for mode A- (power delivered from the PV to the EV).

d) Mode B charging the energy storage

In this mode, the system is configured as follows. The power is delivered from the grid to the energy storage up to the converter's capability of 20 kW. The grid converter is set to balance the DC-link voltages if needed.

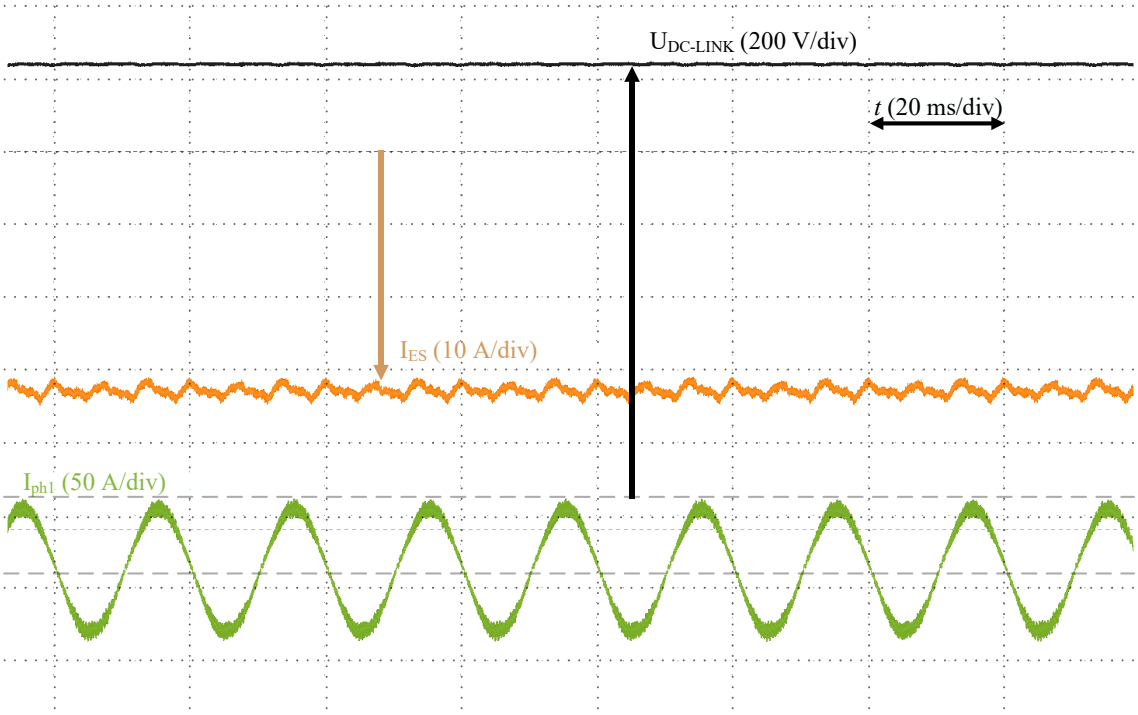

Fig. 9. Exemplary results from mode B, with the power delivered from the grid (20 kW) to the ES (20 kW).

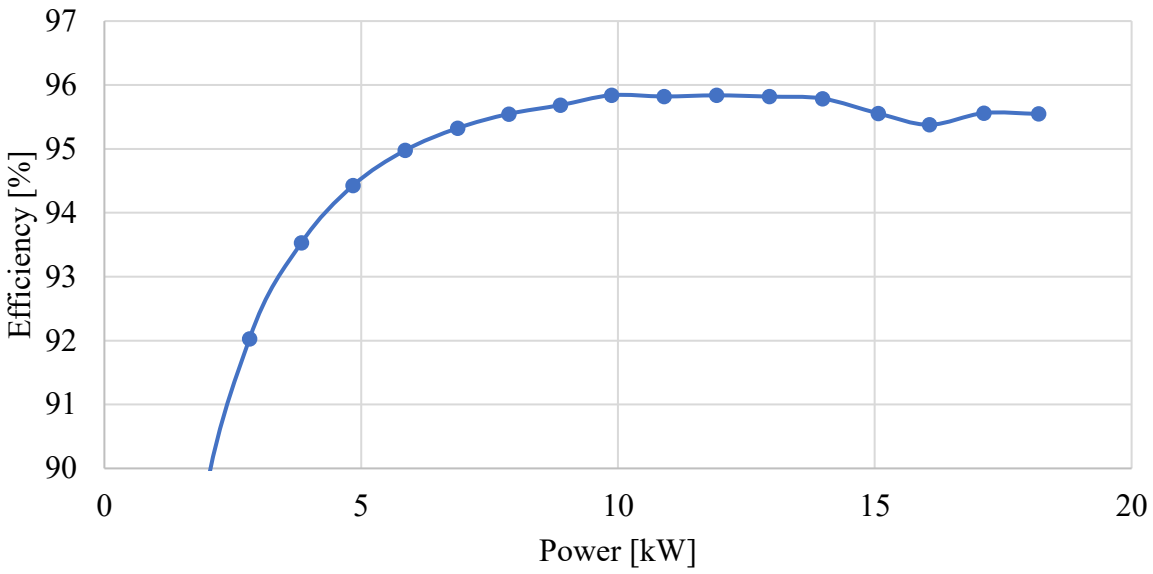

Fig. 10. Efficiency vs. power for mode B (power delivered from the grid to the ES).

e) Mode B+ charging ES from the grid with PV

In this mode variation, the ES is charged from grid and PV. Exemplary results with the ES power of 10 kW, with 10 kW drawn from PV are depicted in Fig. 11. As can be seen, there are slight power fluctuations in the PV converter. However, these are minor and the average power is equal to the set value. Furthermore, the efficiency for various operating points are shown in Fig. 12. Similar figures but for a higher power of ES at 18 kW are depicted in Fig. 13 and 14, respectively.

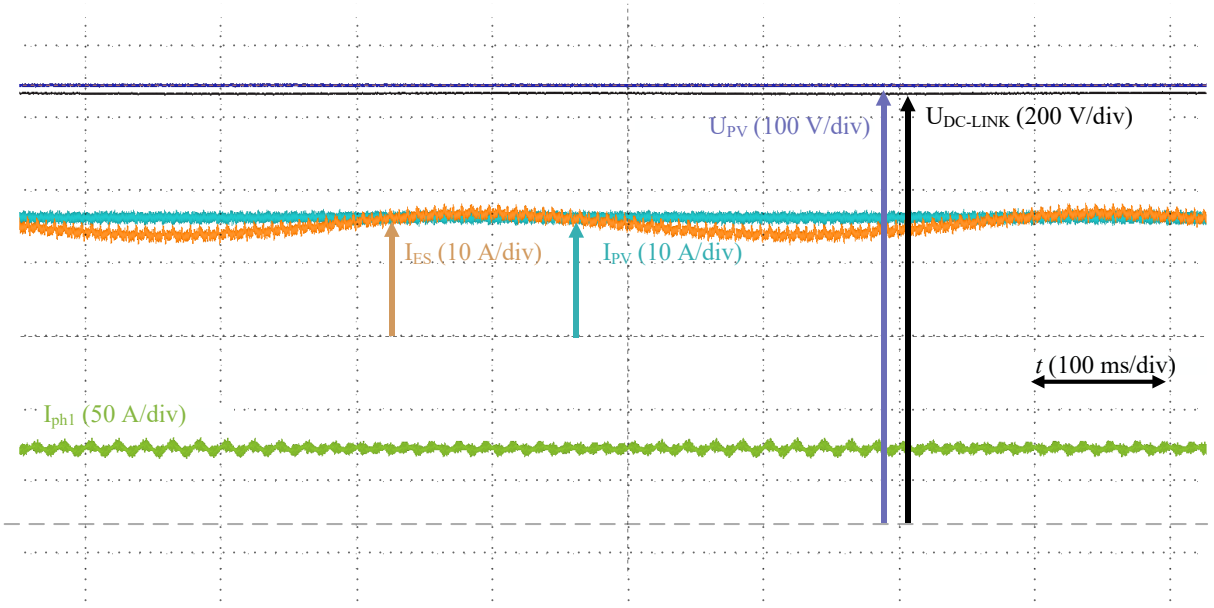

Fig. 11. Exemplary results from mode B+, with the power delivered from and PV (10 kW) to the ES (10 kW).

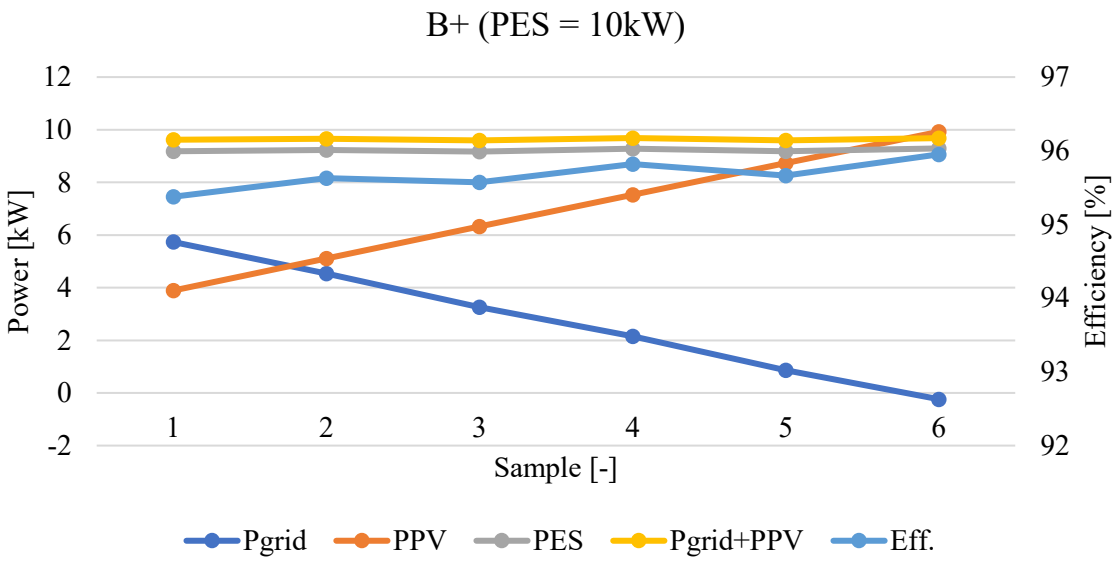

Fig. 12. Power characteristic in mode B+, with the power split varying between the PV plant and the grid (0-5 kW) at a constant load power delivered to the EV at 10 kW.

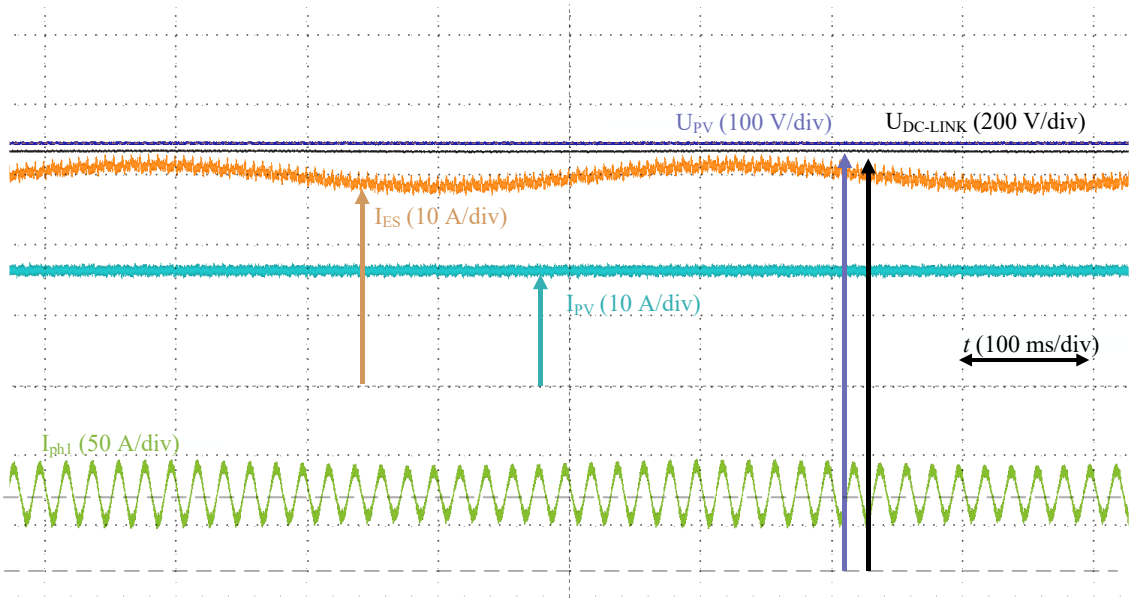

Fig. 13. Exemplary results from mode B+, with the power delivered from the grid (8 kW) and PV (10 kW) to the ES (18 kW).

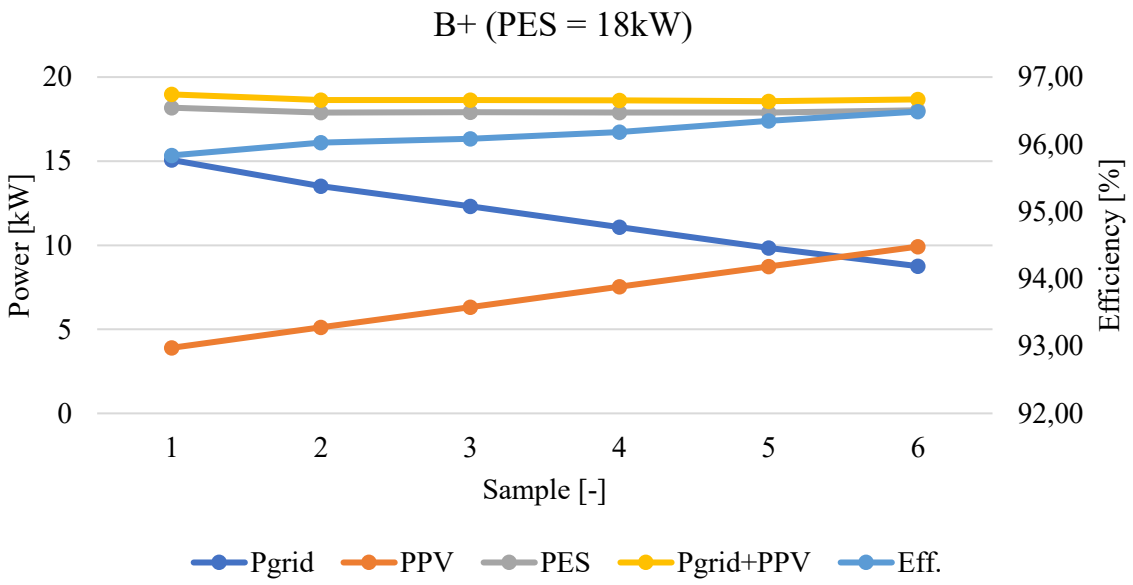

Fig. 14. Power characteristic in mode B+, with the power split varying between the PV plant and the grid (0-9 kW) at a constant load power delivered to the EV at 18 kW.

f) Mode B- charging ES from the PV

In this mode variant, the ES is charged exclusively from the PV plant, whereas the grid converter does not convey any power. Additionally, the grid can be either responsible for balancing DC-link, or completely off, where the ES converter balances the DC-link. This situation, and how does it affect the efficiency, is depicted in Fig. 15.

Fig. 15. Exemplary results from mode B-, with the power delivered from the PV (10 kW) to the ES (10 kW).

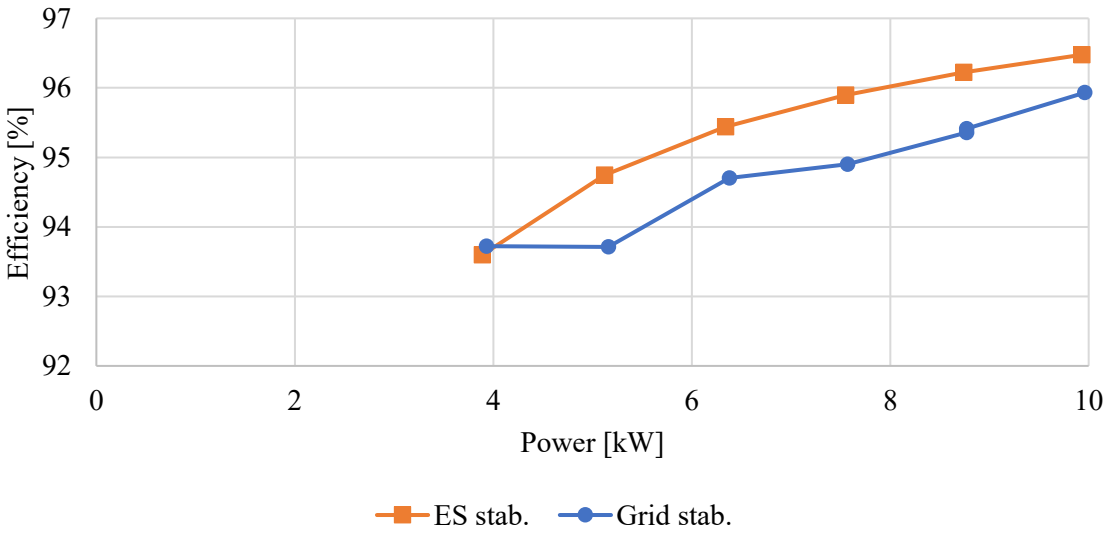

Fig. 16. Efficiency vs. power for mode B- (power delivered from the PV to the ES), for two modes: ES converter stabilizes the DC-link (color 1), grid converter stabilizes the DC-link (color 2).

g) Mode C – fast charging from the grid from the ES and grid and paralleled EV converters

In this mode family, the idea is that the EV converters are connected in parallel and the power can be drawn from various sources. This is the most complicated scenario group, with all the converters from the experimental model possibly cooperating. Therefore, given the limitation of measurement channels, the full efficiency measurement was not possible. Nevertheless, the system has been succesfully tested in the experiments, according to the operating points depicted in Table I.

Table I Test points for the scenario group C/C+/C-

PEV [kW]	2x10				
Pgrid [kW]	10	5	5	0	10
PES [kW]	5	10	5	10	10
PPV [kW]	5	5	10	10	0
Fig.	19	20	21	22	17

Fig. 17 depicts an exemplary results from mode C, with the power delivered from the ES (10 kW) and grid (10 kW) to the EV via parallel connected EV converters (20 kW). As can be seen, the system operation is validated successfully. Furthermore, the efficiency plot for this mode is shown in Fig. 18.

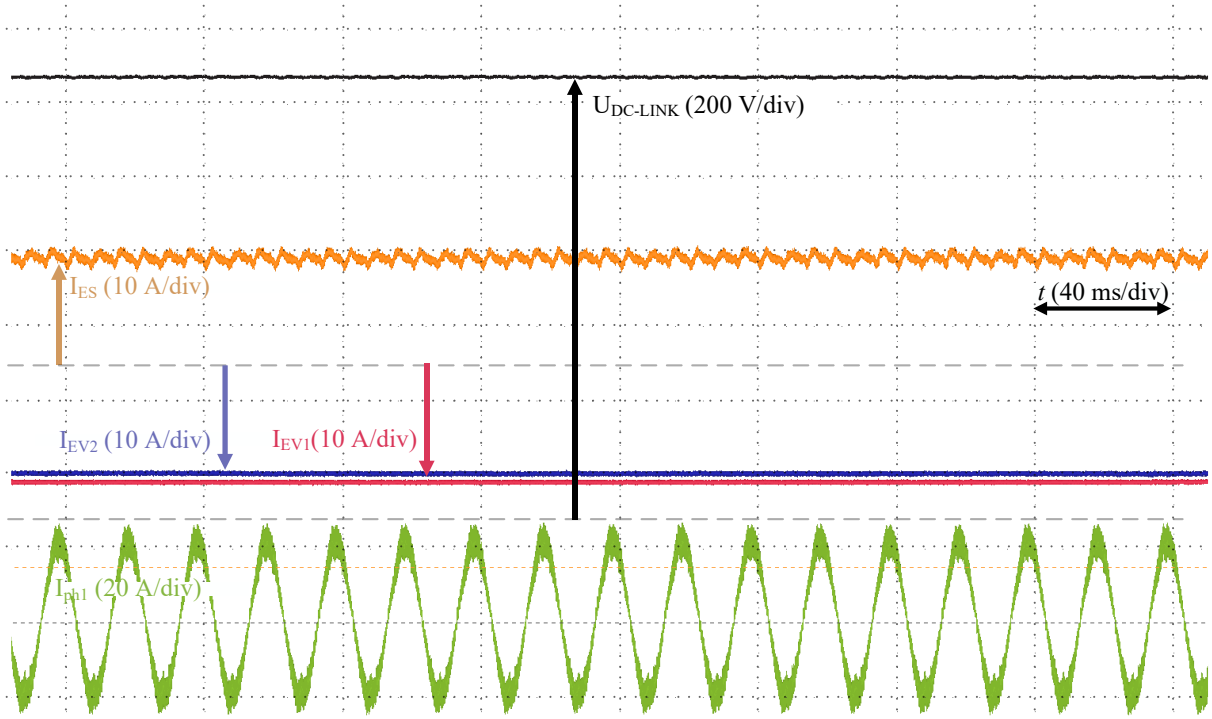

Fig. 17. Exemplary results from mode C, with the power delivered from the ES (10 kW) and grid (10 kW) to the EV via parallel connected EV converters (20 kW).

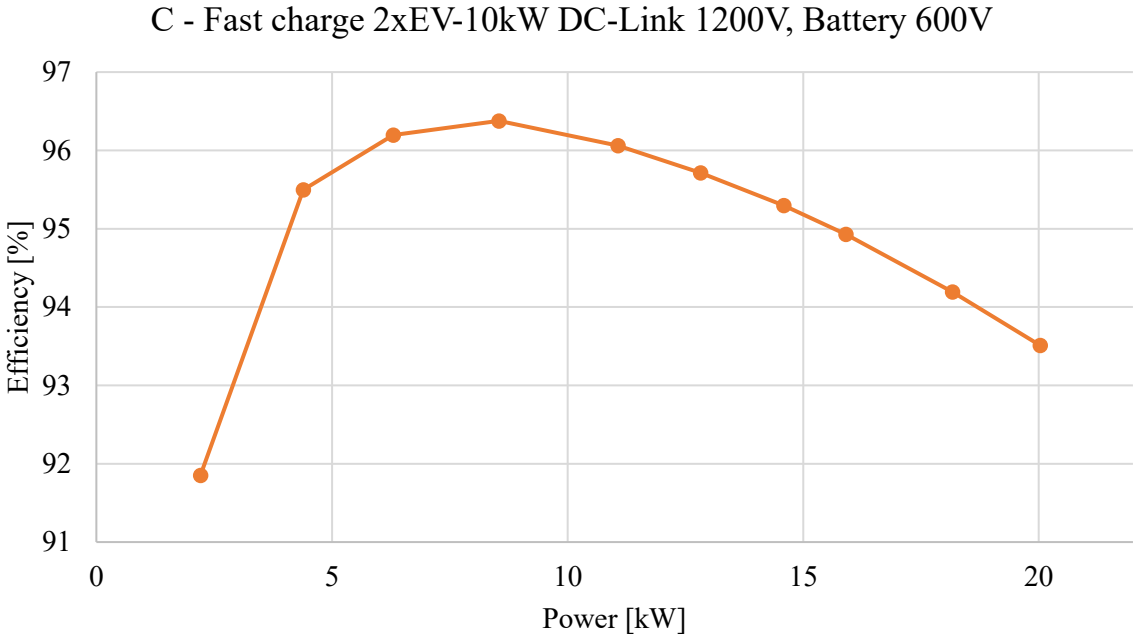

Fig. 18. Efficiency vs. power for mode C (Fast Charge - power delivered from the ES and grid to the EV via parallel connected EV converters).

h) Mode C+ fast charging from the grid and ES with PV

In this variation, the fast charging is supported by additional power drawn from PV. There are several oscillograms depicting this operation, in Fig. 19, 20, 21 and 22, with their respective operating points found in Table I. Again, the operation of the system is successfully verified in the experiments.

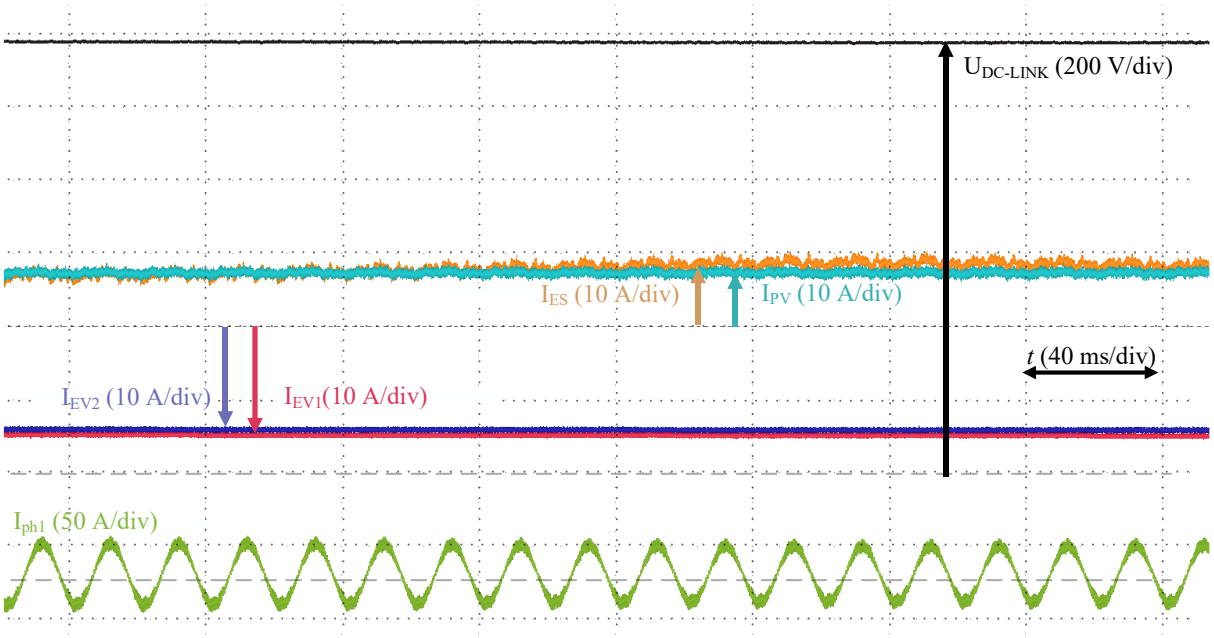

Fig. 19. Exemplary results from mode C+, with the power delivered from the ES (5 kW), PV (5 kW) and grid (10 kW) to the EV via parallel connected EV converters (20 kW).

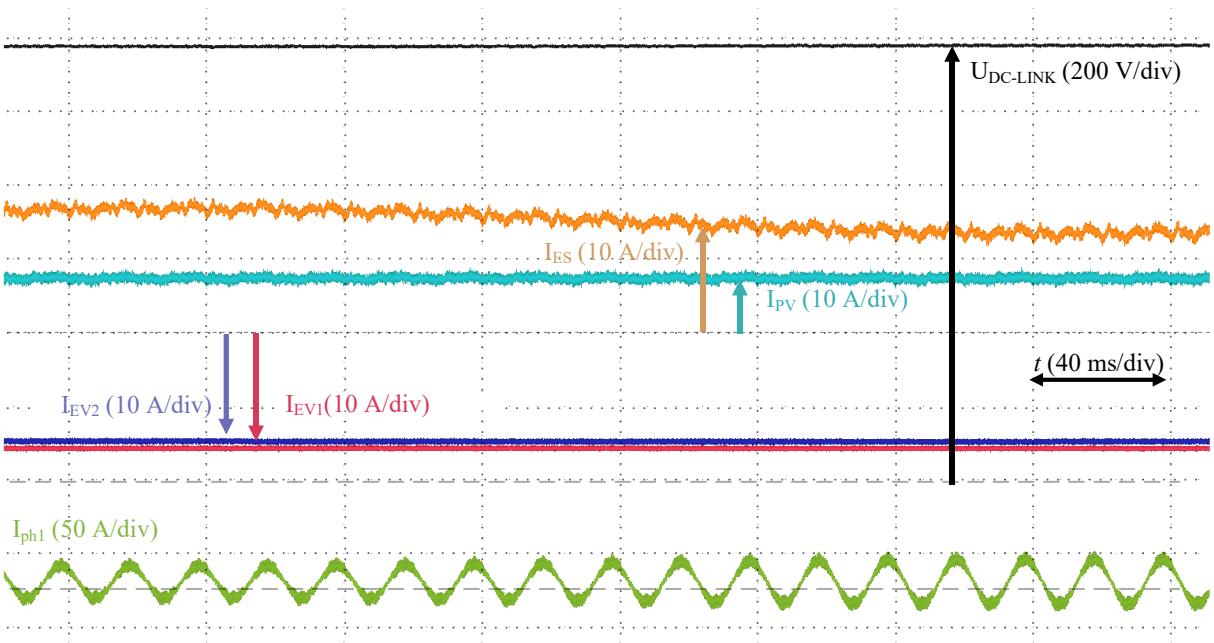

Fig. 20. Exemplary results from mode C+, with the power delivered from the ES (10 kW), PV (5 kW) and grid (5 kW) to the EV via parallel connected EV converters (20 kW).

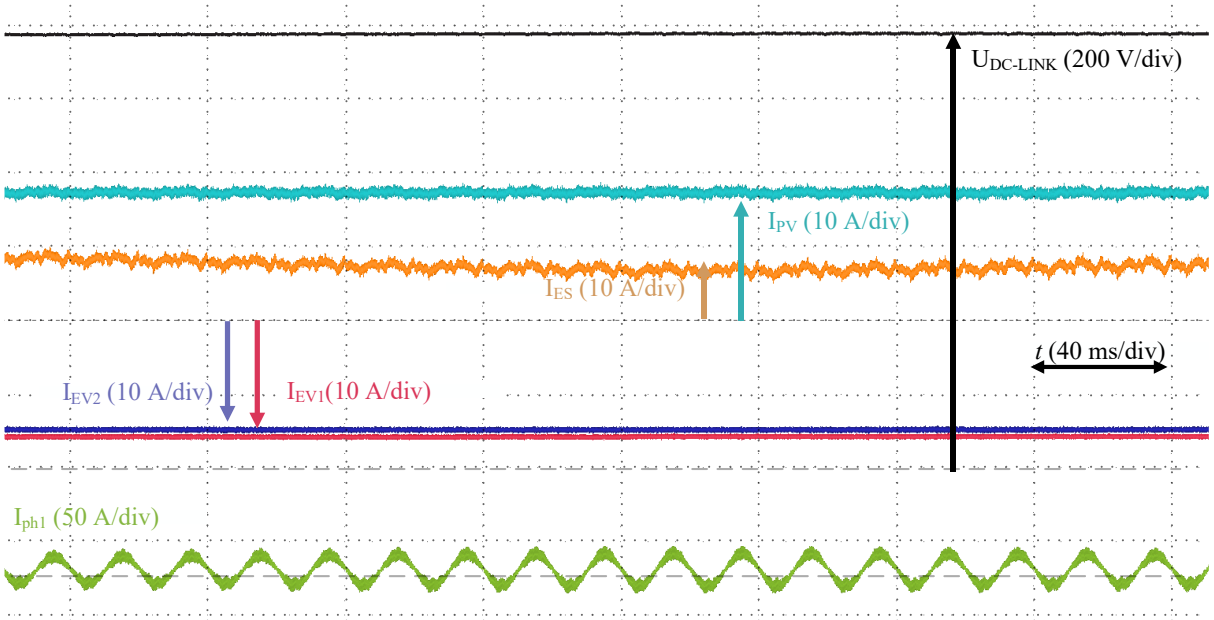

Fig. 21. Exemplary results from mode C+, with the power delivered from the ES (5 kW), PV (10 kW) and grid (5 kW) to the EV via parallel connected EV converters (20 kW).

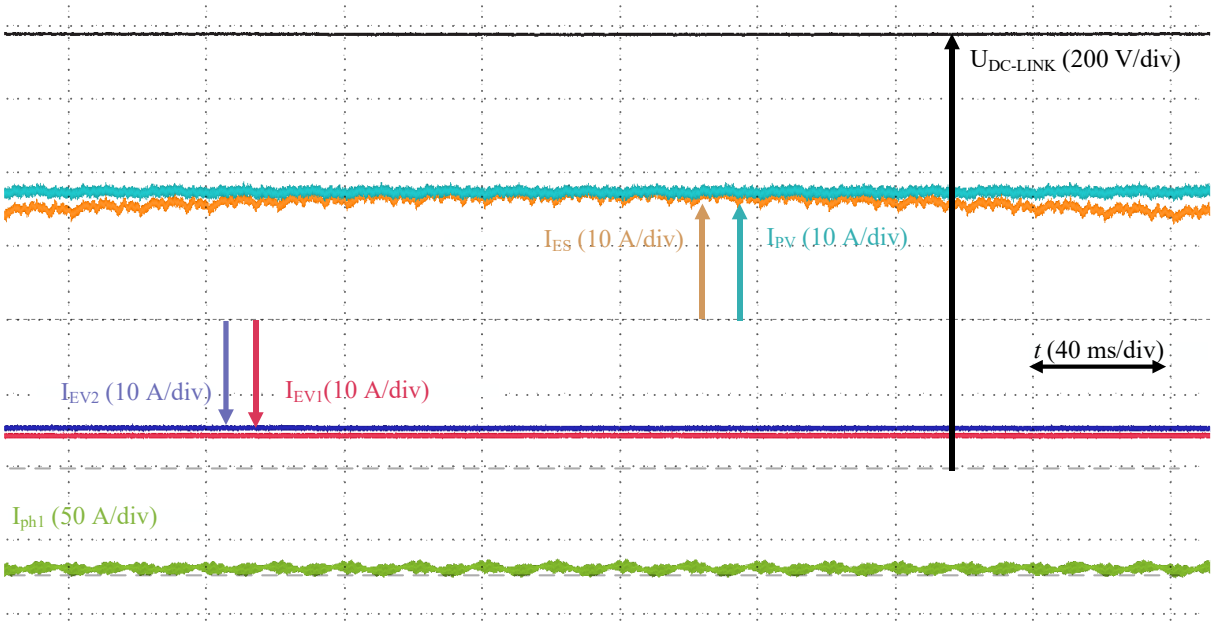

Fig. 22. Exemplary results from mode C+, with the power delivered from the ES (10 kW), PV (10 kW) to the EV via parallel connected EV converters (20 kW).

i) Mode D grid support from the ES

In this mode, the station is oriented at grid support. More specifically, ES is supporting the mains. An exemplary oscillogram from mode D, with the power delivered from the ES to the grid at the level of 18 kW, is depicted in Fig. 23. As can be observed, the system behaves as anticipated. Furthermore, efficiency graph is plotted in Fig. 24, for a varying power of up to roughly 18 kW. As earlier, the efficiency is good, reach nearly 96% for a decent amount of operating range.

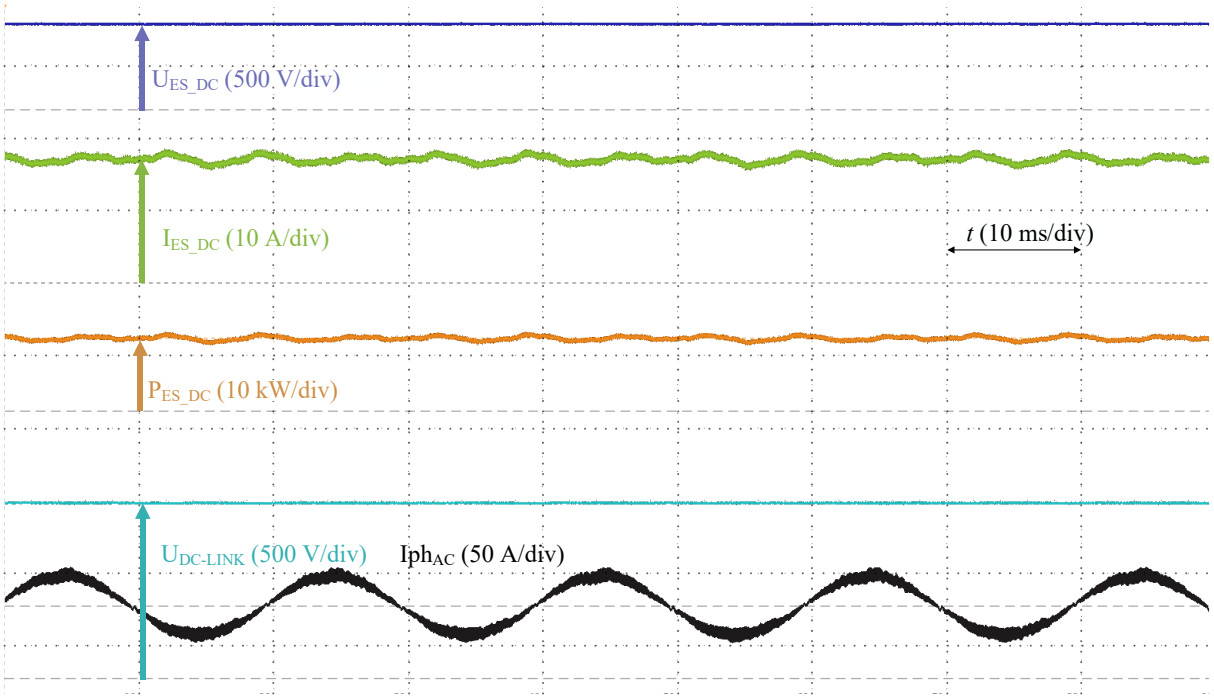

Fig. 23. Exemplary results from mode D, with the power delivered from the ES to the grid (10 kW).

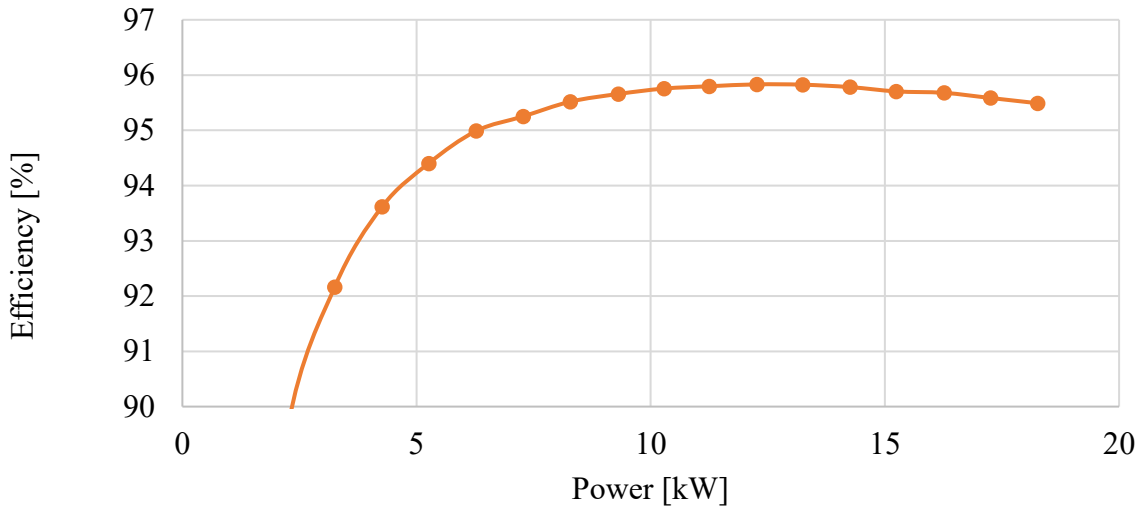

Fig. 24. Efficiency vs. power for mode D (power delivered from the ES to the grid).

j) Mode D+ grid support from the energy storage with PV

In this mode variant, the grid support is enhanced with additional power from the PV, and thus, not only ES delivers the energy. An exemplary oscillogram from mode D+ is shown in Fig. 25, with the power delivered from the ES (5 kW) and PV (5 kW) to the grid (10 kW), while the efficiency can be observed in Fig. 26, where the power characteristic is depicted.

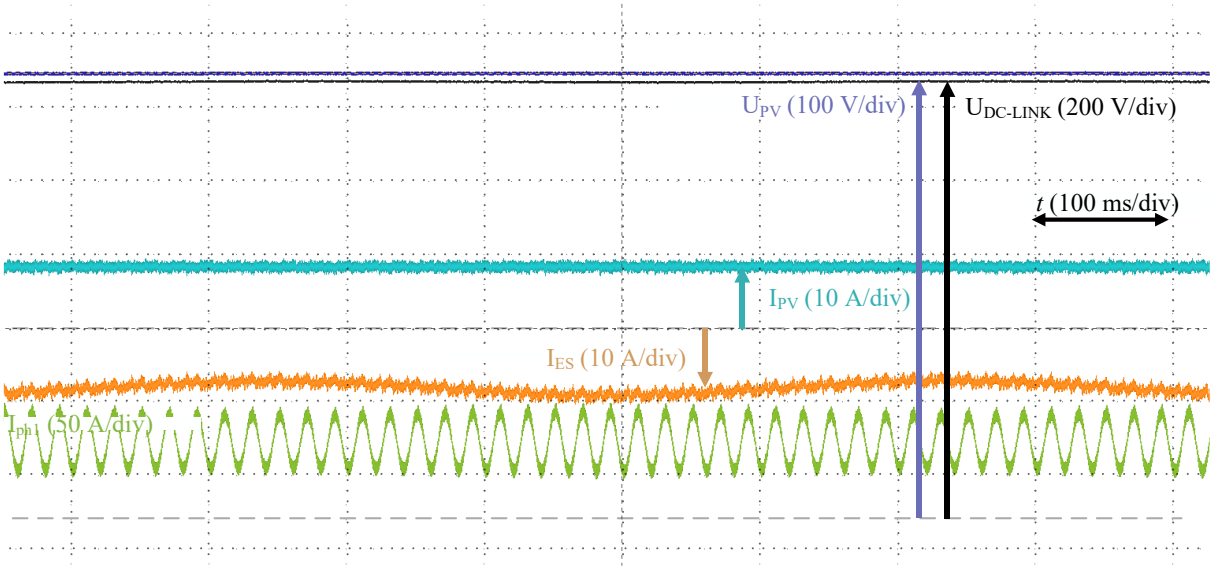

Fig. 25. Exemplary results from mode D+, with the power delivered from the ES (5 kW) and PV (5 kW) to the grid (10 kW).

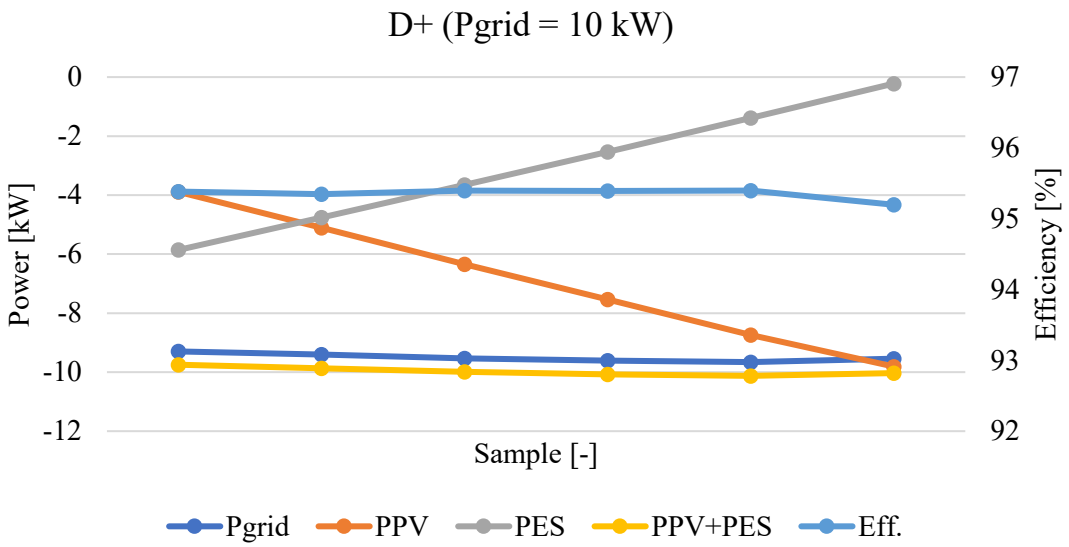

Fig. 26. Power characteristic in mode D+, with the power split varying between the PV plant and the ES (0-10 kW) at a constant load power delivered to the grid at 10 kW.

Another operating point, with a higher power is exhibited in Fig. 27. Here, the power is delivered from the ES (7 kW) and PV (10 kW) to the grid (17 kW), and again, the efficiency can be observed in Fig. 28, where the power characteristic for this operating point is showcased.

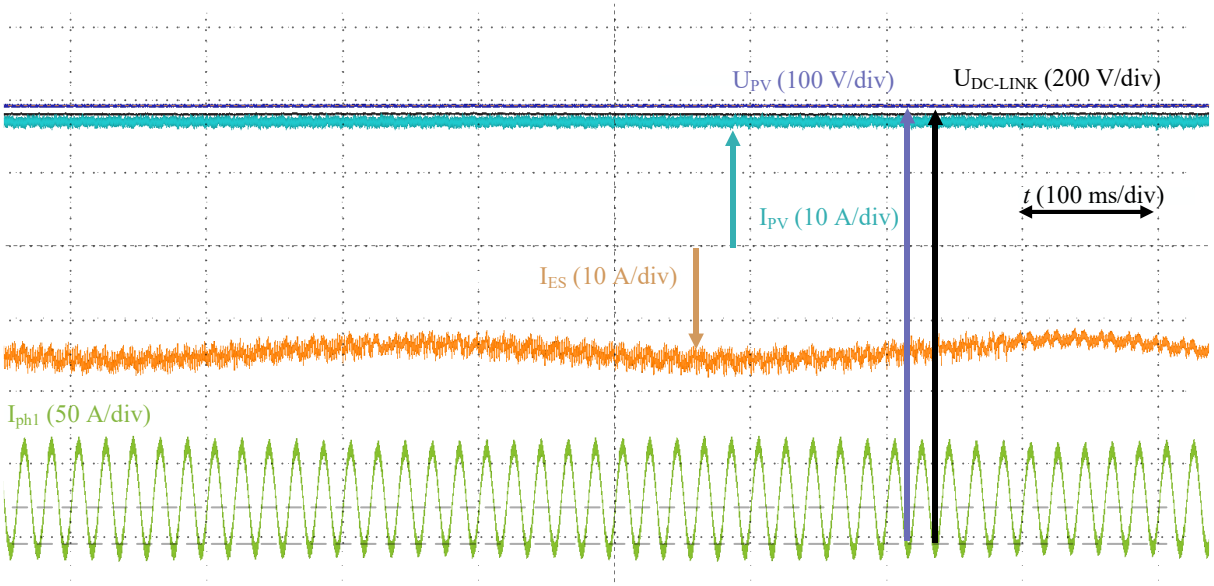

Fig. 27. Exemplary results from mode D+, with the power delivered from the ES (8 kW) and PV (10 kW) to the grid (17 kW).

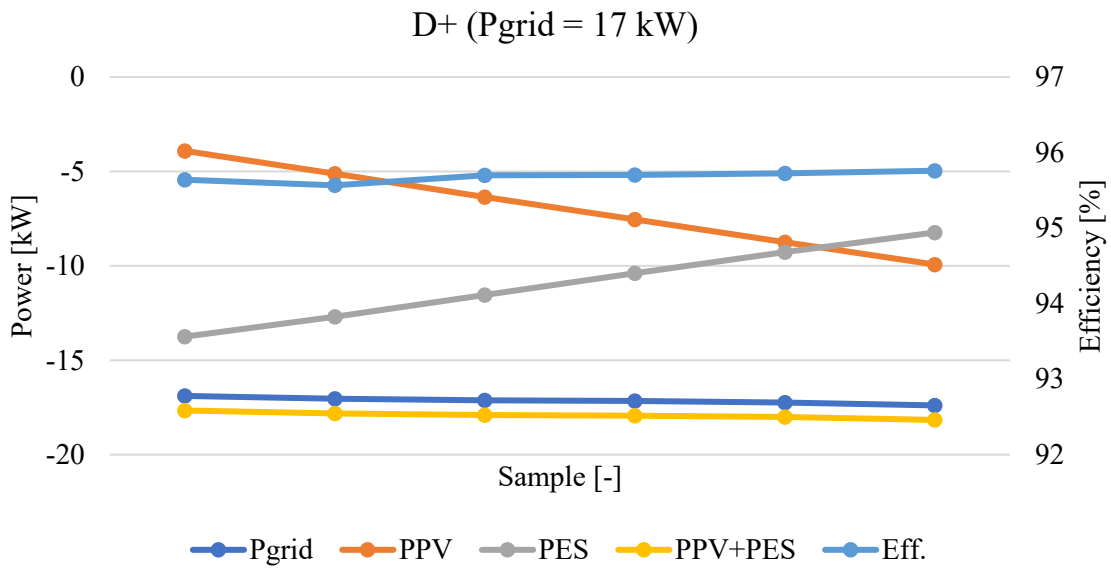

Fig. 28. Power characteristic in mode D+, with the power split varying between the PV plant (4 – 10 kW) and the ES (8 – 14 kW) at a constant load power delivered to the grid at 17 kW.

k) Mode E grid support from the EVs

The next mode E is also focused on grid support. However, in this case, the EVs are source of power. This mode is also commonly referred to as vehicle-to-grid (V2G). Exemplary results from mode E, with the power delivered from the EVs to the grid, at up to 20 kW, are depicted in Fig. 29, while the efficiency plot for this mode is shown in Fig. 30. Furthermore, the power characteristic in time is depicted in Fig. 31, which explains the dynamics of the system in case of the emulation of EV battery discharging. All in all, this mode is also successfully validated.

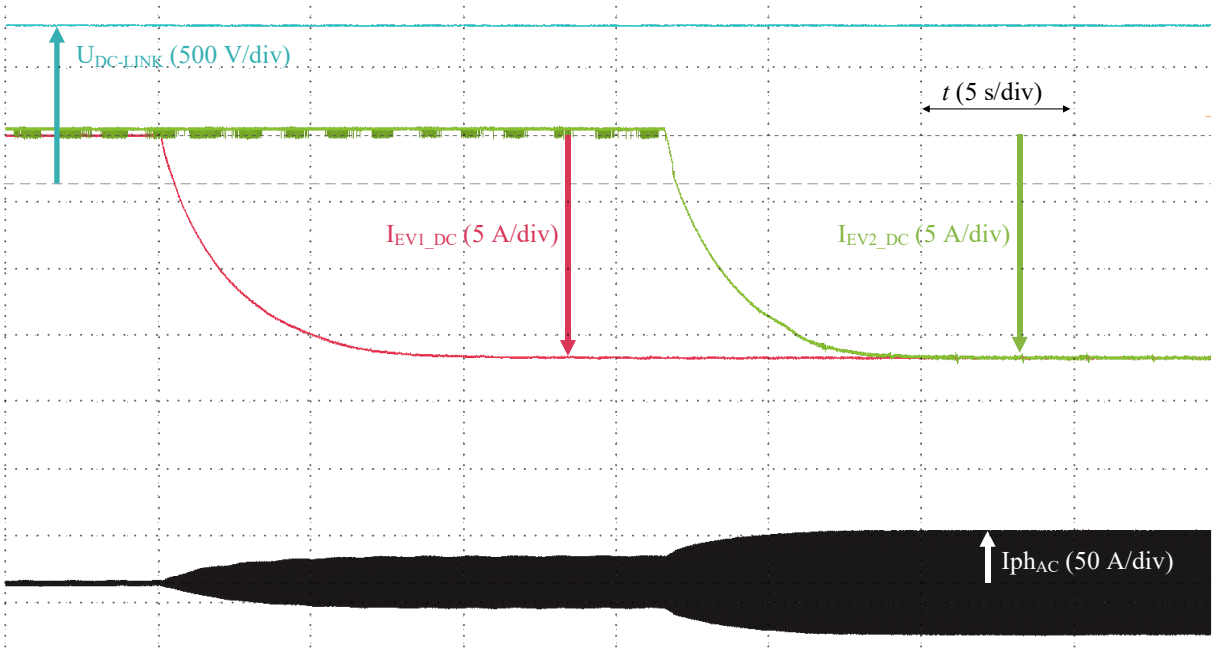

Fig. 29 Exemplary results from mode E, with the power delivered from the EVs to the grid (up to 20 kW).

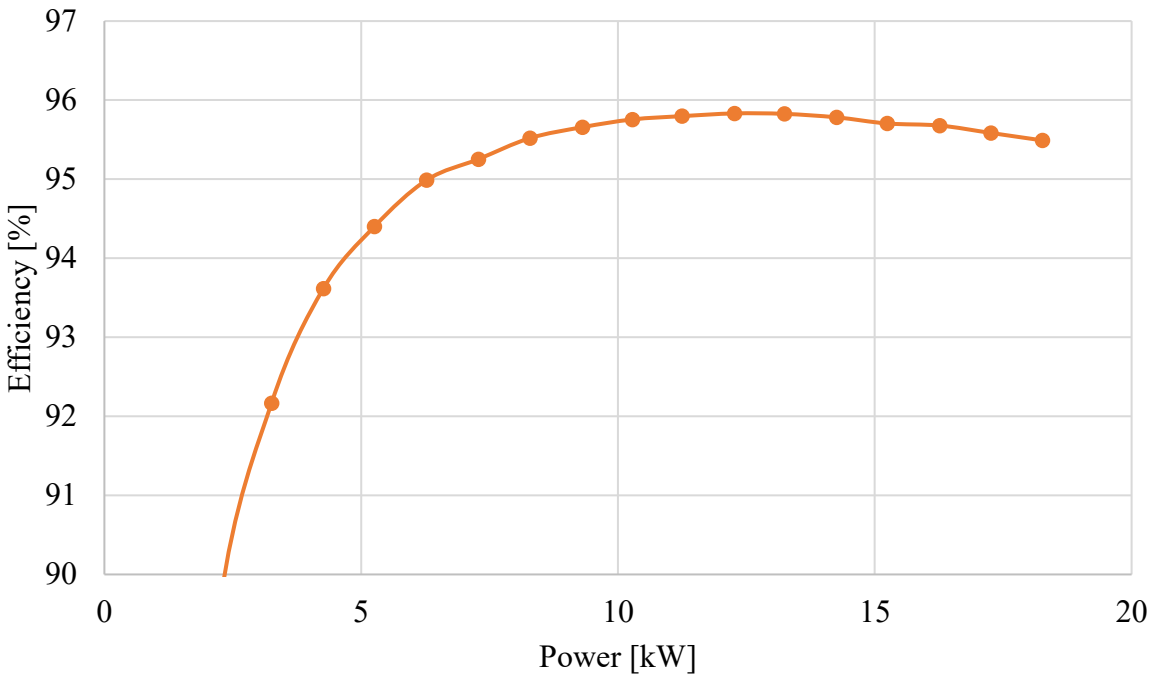

Fig. 30. Efficiency vs. power for mode E (power delivered from the EVs to the grid).

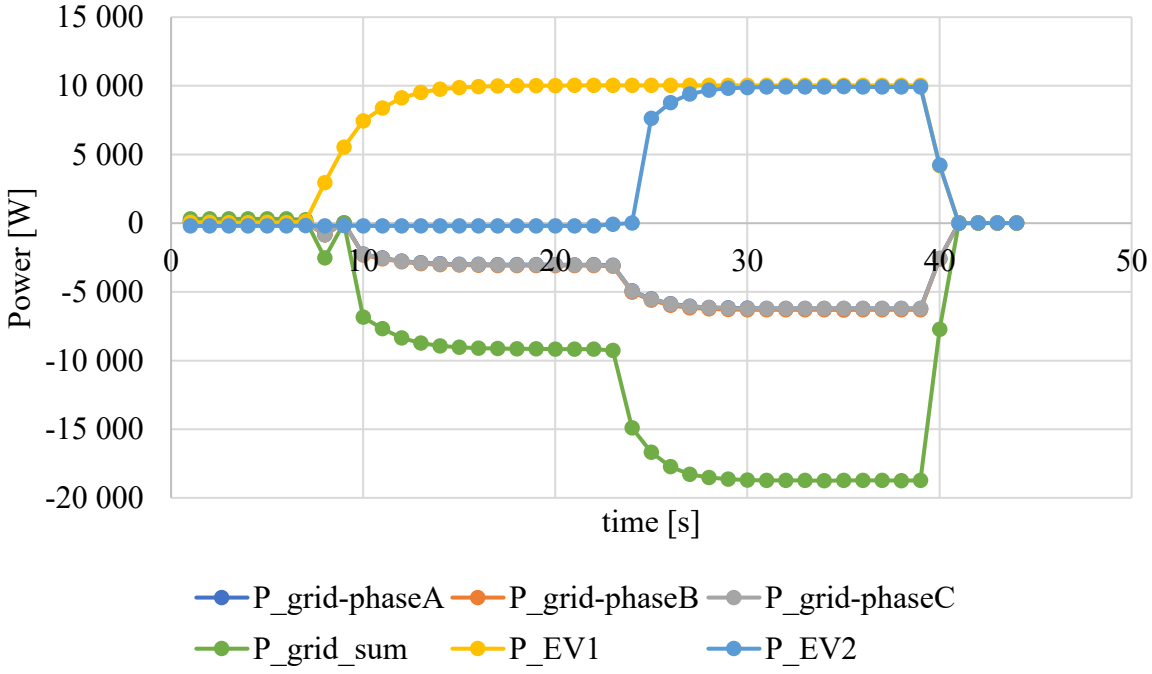

Fig. 31. Power characteristic in mode E, with the power delivered from the EVs to the grid (up to 20 kW).

l) Mode E+ grid support from the EVs with PV

Mode E+ is a PV-enhanced variation of the previously described operation scenario. Here, PV also pushes the power to the grid, along with the EVs. Exemplary results from mode E+, with the power delivered exclusively from the PV to the grid at the power of 10 kW. The power characteristics for varying power split between the EV and PV systems, along with the efficiency measurements, are showcased in Fig. 33. In the end, the hardware experiments successfully validate the system in this mode as well.

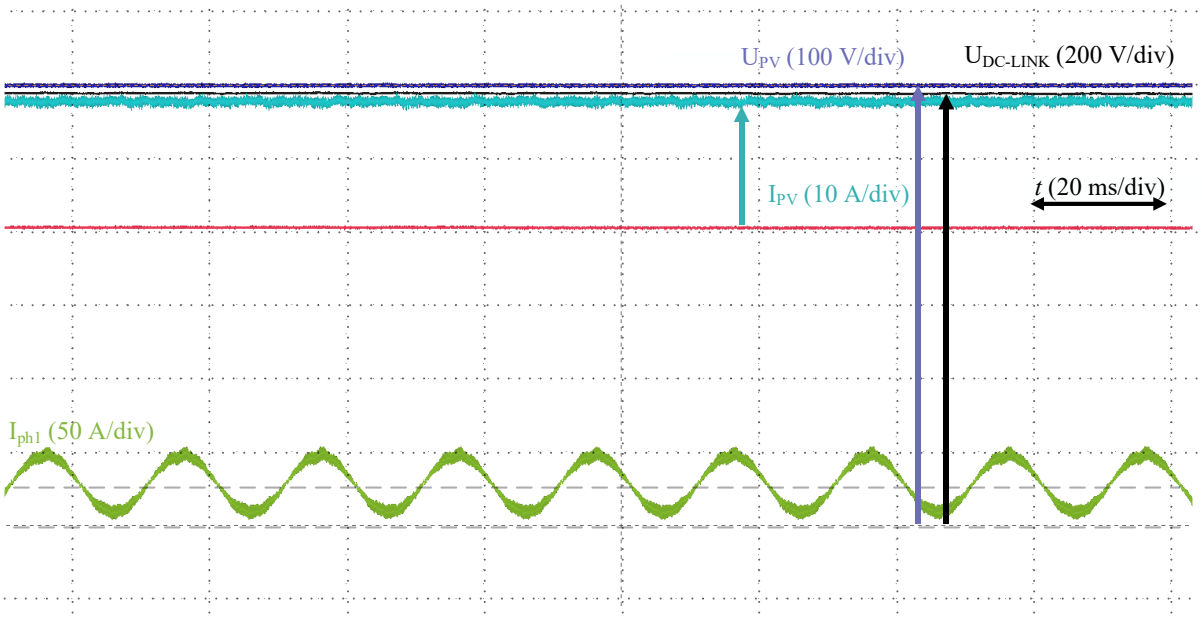

Fig. 32 Exemplary results from mode E+, with the power delivered from the PV to the grid (10 kW).

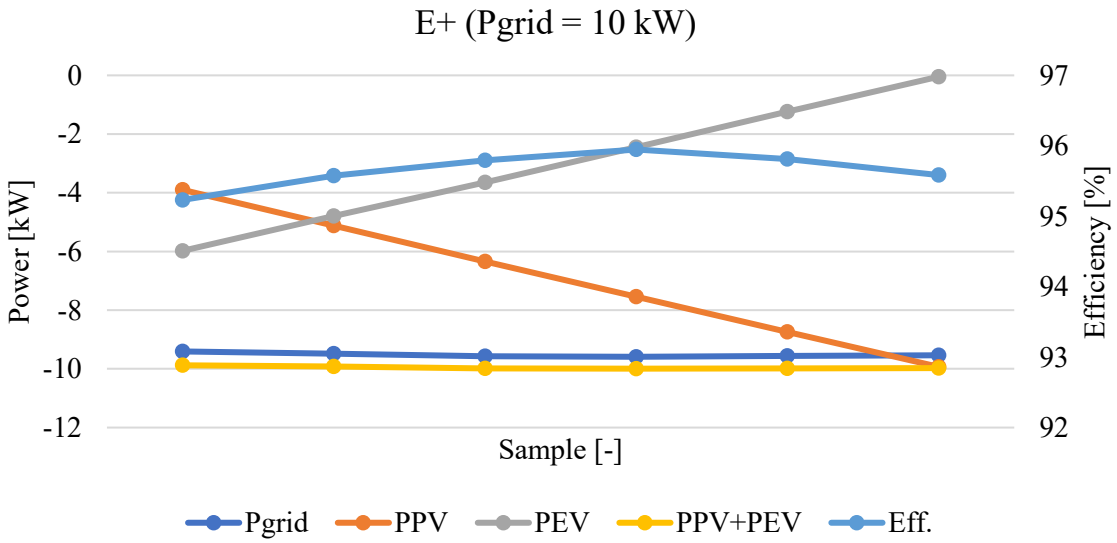

Fig. 33. Power characteristic in mode E+, with the power split varying between the PV plant (4 – 10 kW) and the EV (0-6 kW) at a constant load power delivered to the grid at 10 kW.

m) Mode F island operation; EVs charged from the energy storage

In this mode, the assumption is that grid converter is off, e.g., because of a grid fault. Therefore, when there is a demand for EV charging, the power has to be delivered from the ES. Exemplary result from mode F, with the power delivered from the ES to the EVs at up to 20 kW, is exhibited in Fig. 34, whereas the efficiency plots for one and two EVs connected in parallel are depicted in Fig. 35 and 36, respectively. Once more, the system is positively verified.

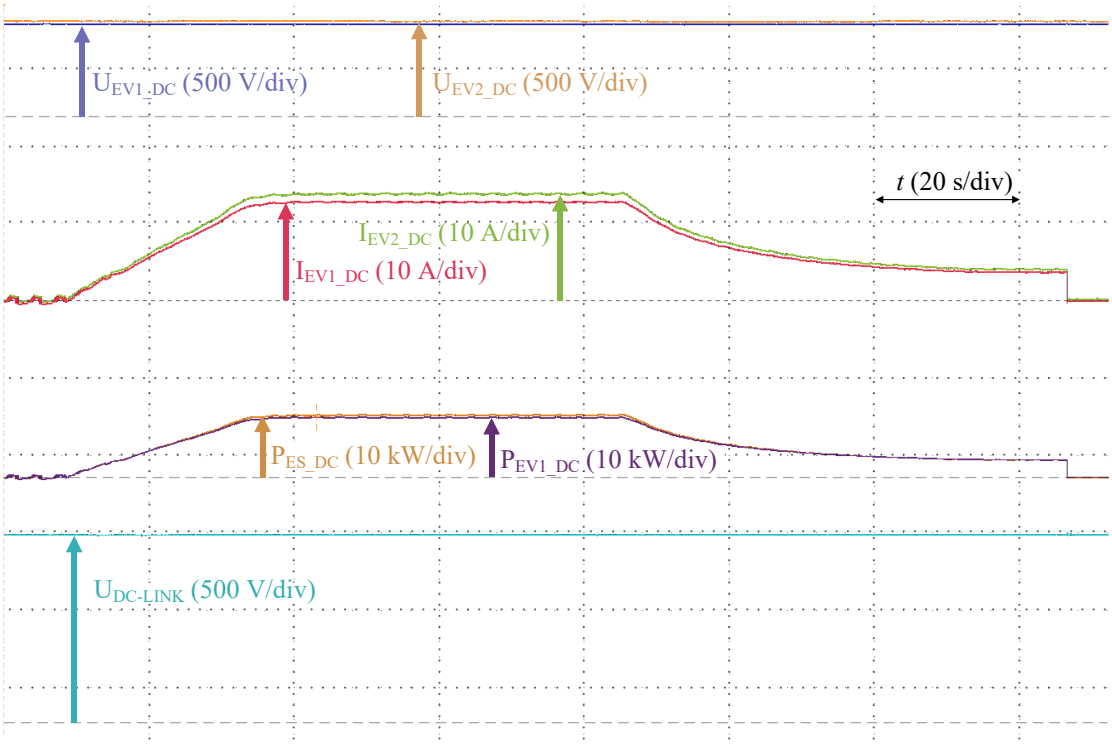

Fig. 34 Exemplary results from mode F, with the power delivered from the ES to the EVs (up to 20 kW).

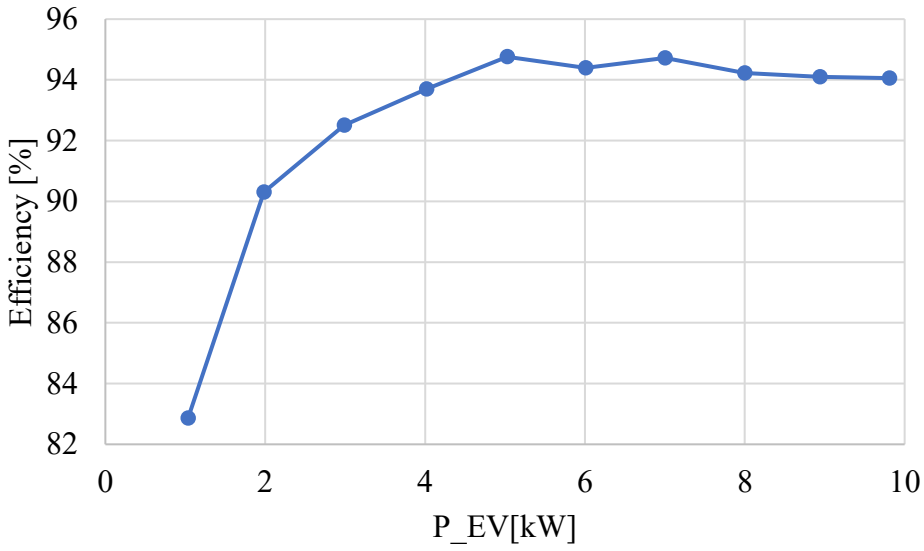

Fig. 35. Efficiency vs. power for mode F (power delivered from the ES to the EV).

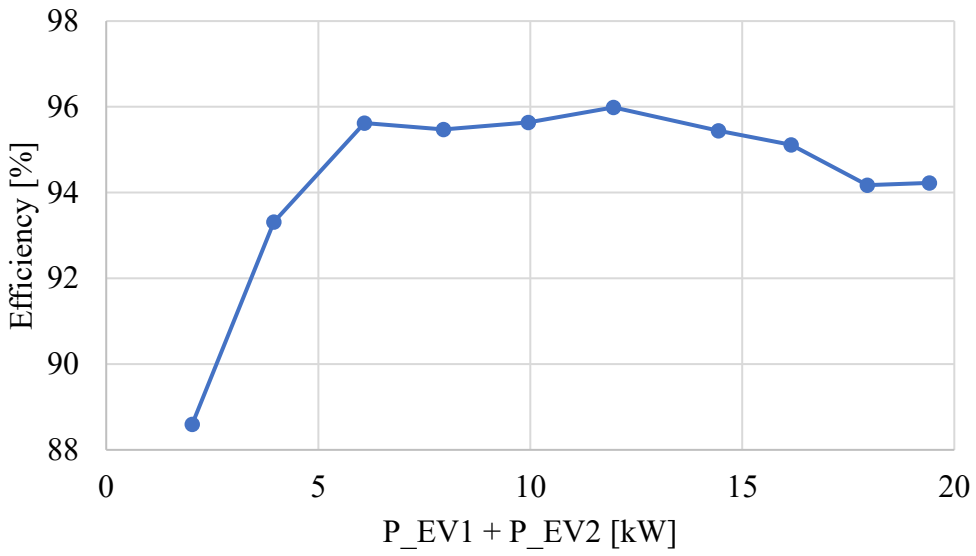

Fig. 36. Efficiency vs. power for mode F (power delivered from the ES to two EVs).

n) Mode F+ island operation; EVs charged from the energy storage with PV

In this enhanced mode, PV also is employed to charge the EVs. Therefore, the power draw is split between the PV plant and the ES. Exemplary results from mode F+, with the power delivered from the PV to the EV at the power of 10 kW is depicted in Fig. 37. Furthermore, specifics on the efficiency and more are showcased in the power characteristic in Fig. 38. All in all, this mode is also successfully validated.

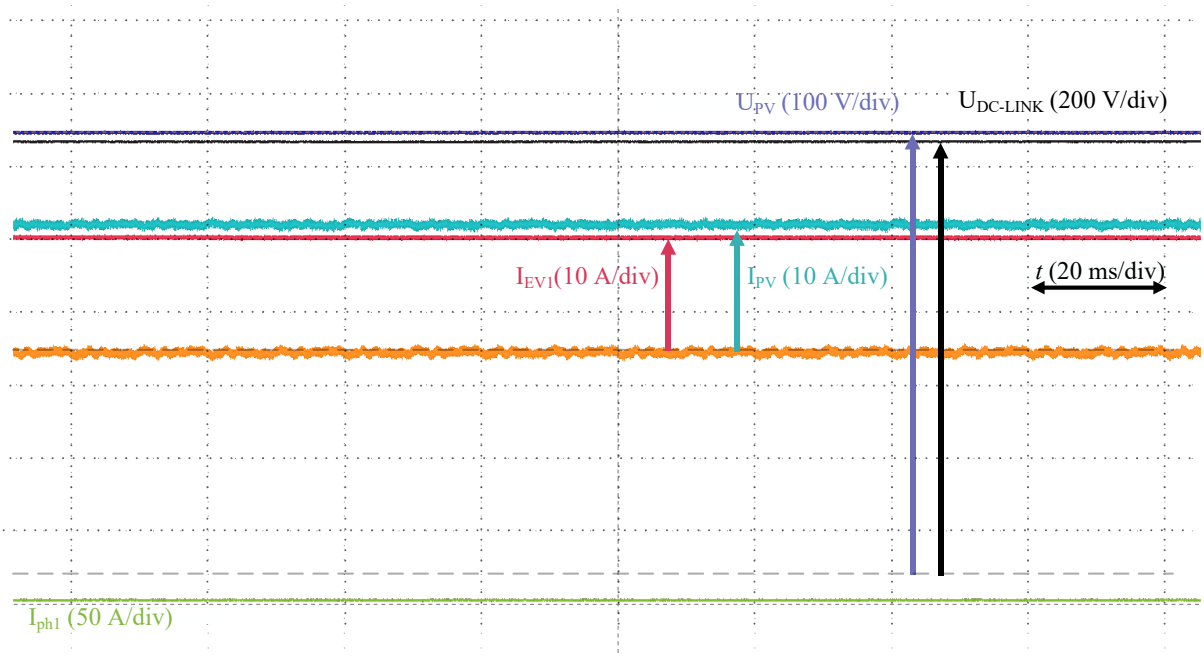

Fig. 37. Exemplary results from mode F+, with the power delivered from the PV the EV (10 kW).

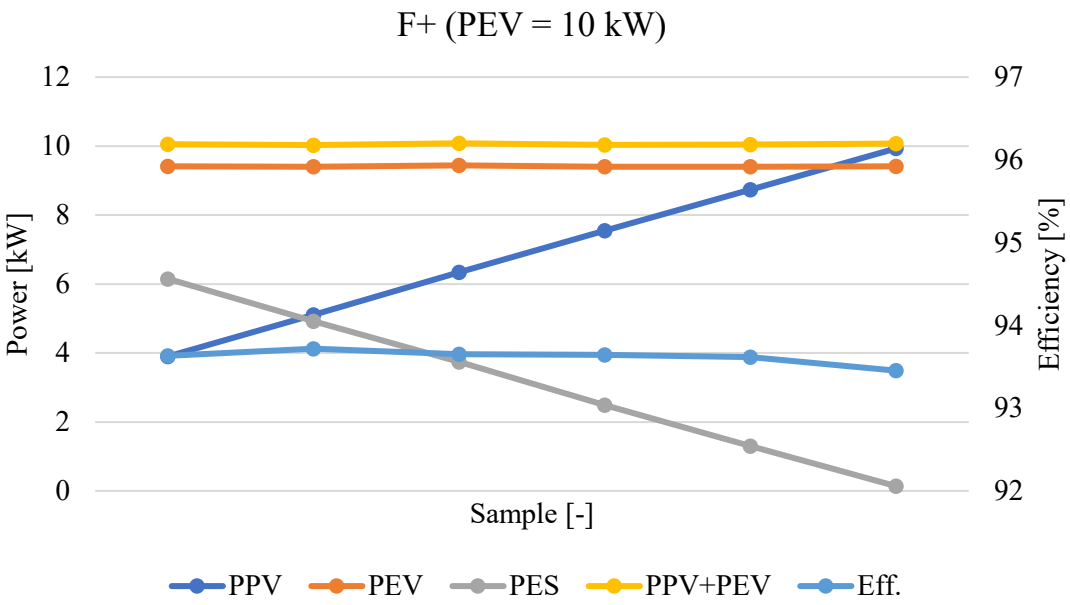

Fig. 38. Power characteristic in mode F+, with the power split varying between the PV plant (4 – 10 kW) and the ES (0-6 kW) at a constant load power delivered to the EV at 10 kW.

o) Mode F- island operation; EVs charged from the PV

Another F mode alternative in the form where only the PV supplies the power can be identified as F- mode. The efficiency characteristic for varying power is depicted in Fig. 39.

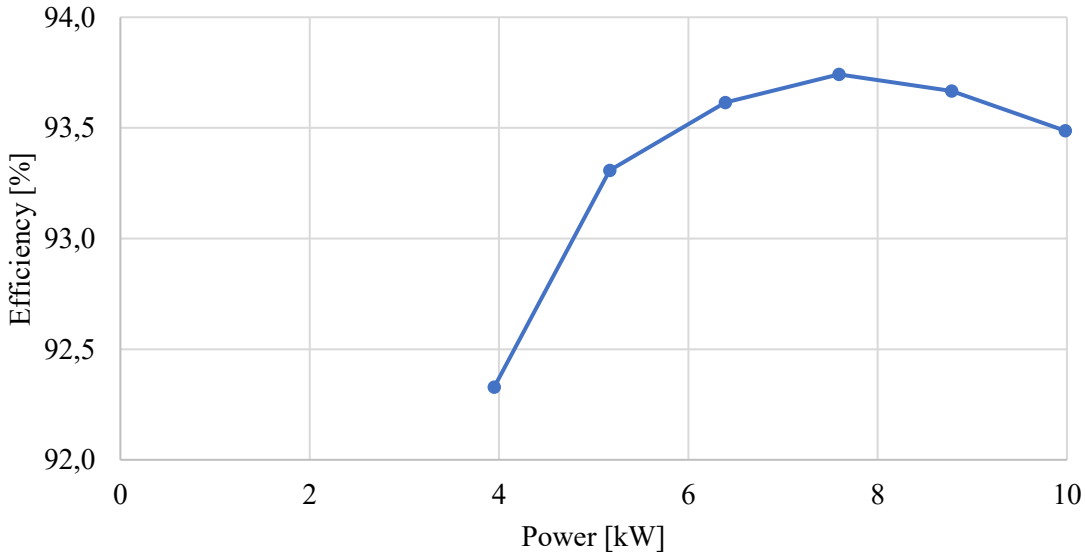

Fig. 39. Efficiency vs. power for mode F- (power delivered from the PV to the EV).

p) Mode G Grid support from the PV

There is also the possibility to deliver the power directly from PV to the grid. For example, when there are appropriate sun conditions that lead to PV power generation but there is no demand from the EV side, and the ES is already fully charged, the energy will be pushed to the grid directly. Thus, additional mode G that has not been considered in the proposal can be considered. The efficiency plot for different operating powers can be found in Fig. 40. Thus, it is shown that also in this mode, the station is provided good performance.

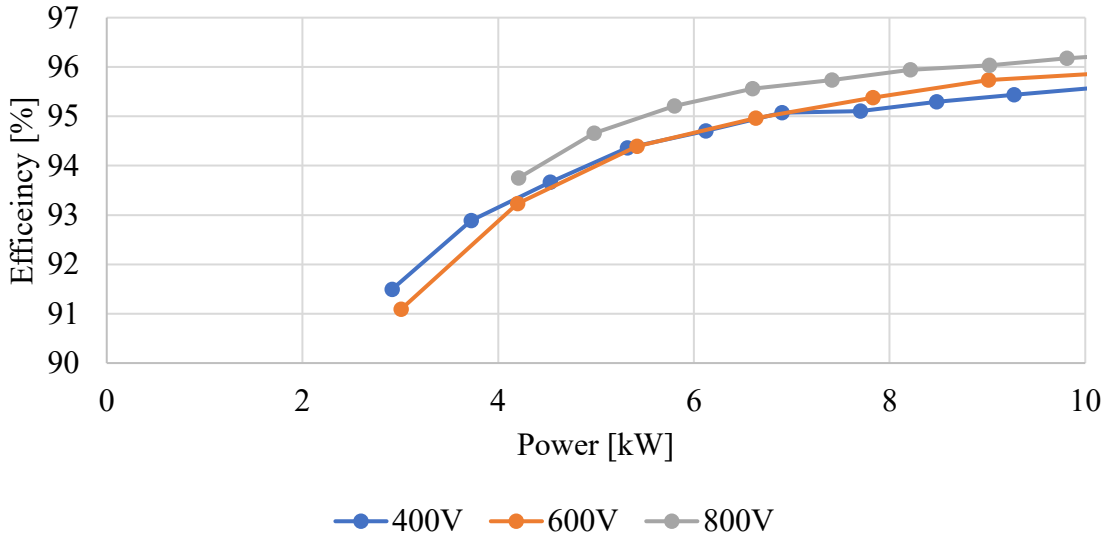

Fig. 40. Efficiency vs. power for mode G (power delivered from the PV to the grid), with several PV voltages.

3. Conclusion

In the deliverable report, the experiments for the complete integrated advanced EV charging system were presented, including the extenstion with an interleaved DC/DC converter integrating a PV plant into the system, leading to more operation modes. The presented experimental results succesfully validate all considered operation modes. Thus, tasks T6.2 – T6.7 are completed, and so is milestone M6 (Completed experiments of the EV charging system).

The specific tasks in more detail:

- T6.2 Investigation of the operation when system is charging two vehicles from the grid in slow charging mode (A);
- T6.3 Verification of the mode B, when slow charging and recharging of the energy storage is considered;
- T6.4 Validation of the fast charging mode, also including the energy storage (mode C);
- T6.5 Testing of the grid support with the use of the storage (D);
- T6.6 Investigation of the vehicle-to-grid operation (E);
- T6.7 Verification of the stand-alone mode, a case with charging during the grid fault (F).